

# Vibrational Sum Frequency Generation Spectroscopy Microscope

Emmanuel Valenton

August 19, 2016

## Abstract

Vibrational sum frequency generation spectroscopy has the benefit of being very surface-specific, aiding in the investigation of a given material's surface chemical and physical properties. As such, the goal of this project was to construct a sum frequency generation microscope that would enable the investigation of surface phenomena on a microscopic scale. Currently, the microscope hardware has been assembled and programmed, and simple spectral images were taken with elastically scattered 532 nm light. These images indicate an image resolution near  $3 \mu\text{m}$ .

## I Introduction

The importance of surfaces in chemical and physical phenomena is demonstrated by the fact that many of these processes occur at this location rather than in the material bulk. One prominent example is corrosion—a common chemical reaction which occurs on the external boundary of metals and other materials rather than inside the material. The extent of the destructive effects of corrosion on a metal depend crucially on the properties of the metal's surface. Such dependence allows steel, for example, a strong metal that is nonetheless very susceptible to oxidation, to be widely used for structural applications provided that its surface is coated by an inert surface such as zinc oxide, for the case of galvanized steel.

Despite its importance, there is difficulty in investigating the surface of a given substance—a difficulty that is attributed to the fact that the surface only makes up a small fraction of the total material. As a result, the bulk-specific signal often dwarfs the surface specific one for many forms of traditional spectroscopy—such as Beers Law spectroscopy. One solution is presented by vibrational sum frequency generation (SFG) spectroscopy. This technique utilizes the non-linear effect where if two laser beams of different frequency coincide spatially and temporally on a surface, not only will reflected and diffracted light result, but an additional beam of light will be created at the point of incidence whose frequency is the sum of the previous two. The attributes that make this non-linear method very attractive include surface-specificity, since the resulting signal is modulated primarily by the surface, and output signal uniqueness, since the signal's frequency is different from that of the incoming beams.

To put it formally, when a molecule (or atom) is struck by a beam of electromagnetic radiation, the electric field of the beam causes the molecule to polarize, resulting in a momentary dipole which oscillates with the oscillating electromagnetic wave. This phenomenon forms the basis for processes such as light scattering. While for low intensities of light the polarization may be approximated as being linearly proportional to the electric field, at high intensities this linear relationship breaks

down and higher order terms are needed:

$$\mathbf{P} = \epsilon_0 \chi \mathbf{E} \quad (1)$$

$$\mathbf{P} = \epsilon_0 \left( \chi^{(1)} \mathbf{E} + \chi^{(2)} \mathbf{E}^2 + \chi^{(3)} \mathbf{E}^3 \dots \right) \quad (2)$$

$\mathbf{P}$  is the polarization vector,  $\chi$  is the molecular susceptibility tensor,  $\epsilon_0$  is the vacuum permittivity,  $\mathbf{E}$  is the electric field vector, and the superscripts in parenthesis indicate the order (first order correction, second order correction, etc)[1]. Now, for the case of two different beams of light striking the same molecule, the incoming electric field could be approximated as a linear combination of the two original beams,

$$\mathbf{E} = \mathbf{E}_0 \cos(\omega_0 t) + \mathbf{E}_1 \cos(\omega_1 t) \quad (3)$$

where  $\omega$  is the frequency of the light and  $t$  is time. Taking the resulting electric field and plugging into the second order term, it is found that the second order correction is as follows:

$$\begin{aligned} \mathbf{P}^{(2)} = \frac{1}{2} \epsilon_0 \chi^{(1)} & (\mathbf{E}_0^2 + \mathbf{E}_1^2 + \mathbf{E}_0^2 \cos(2\omega_0 t) + \mathbf{E}_1^2 \cos(2\omega_1 t) + 2\mathbf{E}_0 \mathbf{E}_1 \cos((\omega_0 - \omega_1)t) + \\ & 2\mathbf{E}_0 \mathbf{E}_1 \cos((\omega_0 + \omega_1)t)) \end{aligned} \quad (4)$$

This summation indicates that a number of non-linear effects are taking place such as second harmonic generation and that the molecule is re-radiating light of different frequencies. That said, the origin of sum frequency generation can be found in one of these terms,

$$\mathbf{P} \propto \mathbf{E}_0 \mathbf{E}_1 \cos((\omega_0 + \omega_1)t) \quad (5)$$

where the other terms (and the other non-linear effects) are neglected. Thus, it is seen that the polarization vector oscillates at the sum of the frequencies of the incoming beams, resulting in a coherent emission of light whose frequency is the sum of the previous two.

With this in mind, the goal of this project was to build a spectroscopic microscope that would produce images using sum frequency generation. Such device would enable the study of the chemical composition and molecular orientation of surfaces. This information would be useful in applications such as investigating the degradation of plastic exposed to the natural elements as well as investigating the surface properties of catalysts.

## II Experimental

Below is described the full design of the instrument starting first with the laser pulses for sum frequency generation (see Figure 1). A femtosecond(fs) oscillator is used to create 800 nm laser pulses, which are then amplified using a fs amplifier. A fraction of the amplified light is directed towards a Frequency Resolved Optical Gating (FROG) device for pulse characterization while the rest of the 800 nm light is fed into a TOPAS device allowing the light to be converted into mid-range IR laser pulses. These pulses are then directed towards a dichroic mirror.

On a separate path, a picosecond (ps) oscillator is used to create 532 nm laser pulses that are then amplified and directed towards the same dichroic mirror. The ps oscillator is synchronized with the fs oscillator using an RF 100 MHz master clock allowing the pulses to coincide temporally. After reflecting off the dichroic mirror, the 532 nm light travels co-linearly through a second dichroic mirror to enter the reflective objective of the microscope.

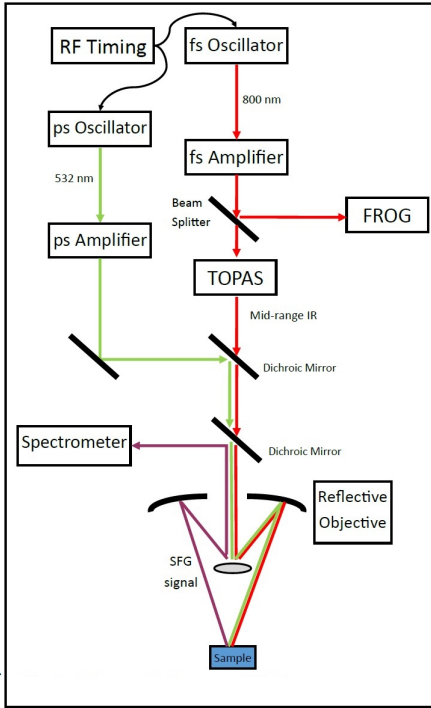


Figure 1: Laser diagram of sum frequency generation setup.

The objective focuses the light onto the sample, yielding an SFG signal which is recaptured by the objective. The SFG signal reflects off the second dichroic mirror into a spectrometer for analysis.

The microscope itself consists of an Olympus optical microscope with a computer controlled xy-stage and a gold-coated wide wavelength range reflective objective (See Figure 2). The objective is crucial to the operation of the microscope since it is capable of reflecting light ranging from visible to mid-infrared. Thus, the incoming 532 nm and mid-IR laser pulses may be focused to a pinpoint spot on the sample and the resulting SFG signal, which is shifted up in frequency, may be captured without significant loss of light. Likewise, the xy-stage is also an essential component of the microscope. Since the goal is to obtain SFG signals, the device cannot resolve images like a standard optical microscope. Instead, the incoming 532 nm and mid-IR lasers are focused on a point on the sample and an SFG spectrum is taken of that spot. Then, the xy-stage is moved a short distance, with the shortest distance possible being  $0.1 \mu\text{m}$ , so that the lasers are focused on a new spot and another SFG spectrum is taken.

In this manner, the SFG microscope rasters across the entire sample and then the resulting frequency-resolved spectra are collected into a hyperspectral image.

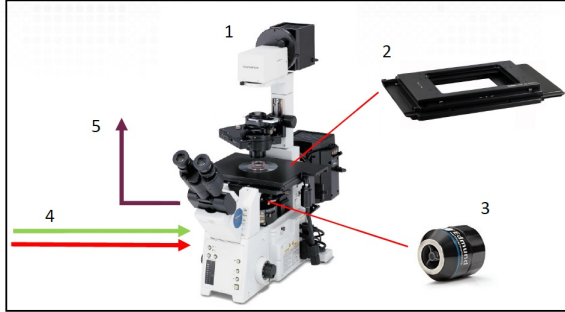


Figure 2: Exploded view of microscope: (1) optical microscope, (2) xy-stage, (3) wide wavelength reflective objective, (4) incoming tunable IR and 532 nm laser pulses for sum frequency generation, (5) SFG signal out.

### III Results

A number of stages have been achieved towards the goal of constructing the microscope. First, the control software has been finished (see Figure 3), which would control and coordinate the xy-stage and spectrometer camera. The user would enter in the parameters for the camera as well as the spatial range of the sample that is to be imaged and then the program would then compute

the raster path, adjust the camera, move the stage, and acquire data. The raw camera data is displayed in real-time as the acquisition process is progressing, and once finished, the program stores the data away in a file. The program also allows the user to take an SFG spectrum of a single spot on the sample should there be a region of interest. Together, the program and stage are capable of movements as small as  $0.1\text{ }\mu\text{m}$ .

After the hardware was assembled and the program installed, the SFG microscope was tested with a white diffusive reflector as a sample target and with just a single 532 nm laser beam running through the setup. The purpose was not to acquire an SFG spectrum or image, but to ensure that the xy-stage operated as expected and that the program was accurately recording data from the spectrometer. Assuming that a constant amount of light is reflected off diffusive reflector, regardless of sample position, any difference between the resulting spectra would indicate an error in the control software or laser setup. After performing the acquisition, a large peak was seen in each spectrum (see Figure 4), which may be attributed to elastic scattering from the sample by the 532 nm beam. The relative closeness of the 532 nm peaks for each spectrum indicates that the control software is properly handling the data and that the laser setup is aligned properly.

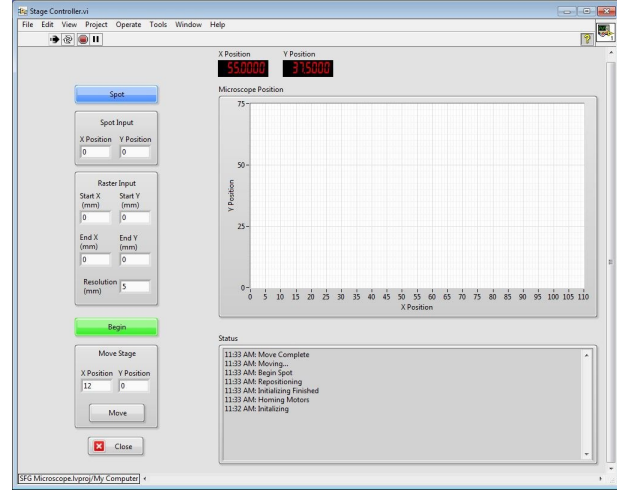


Figure 3: Front Panel of SFG microscope control software

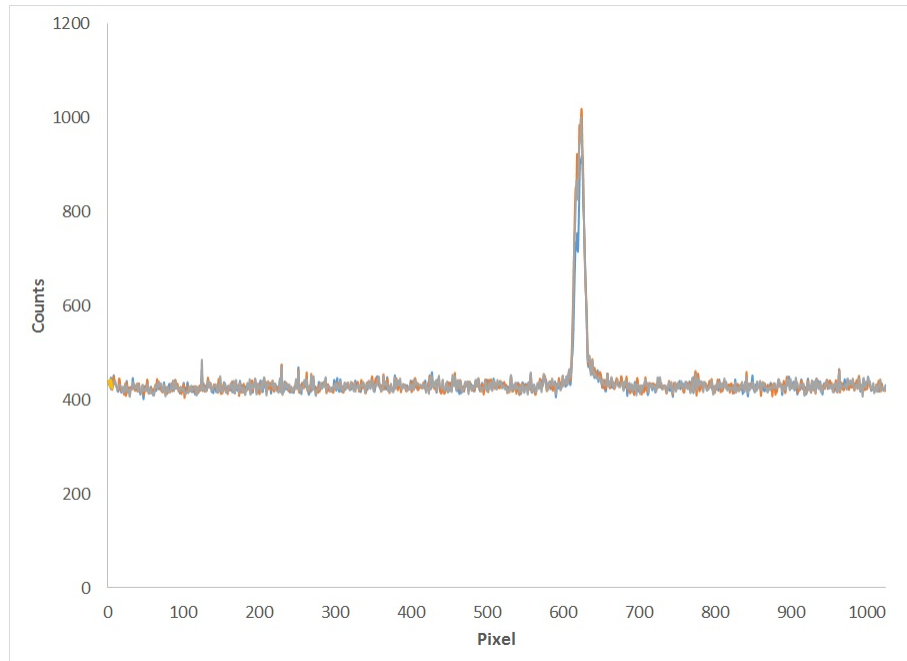


Figure 4: Spectra of white diffusive reflector under 532 nm laser, taken at different stage positions.

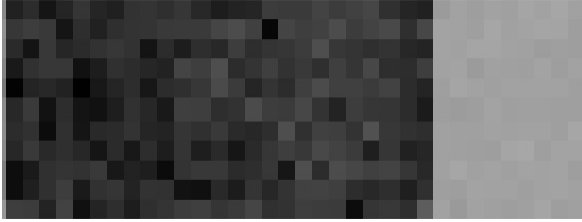


Figure 5: Image of paper edge taken under 532 nm laser light. Actual sample is  $990\mu\text{m} \times 300\mu\text{m}$ . Light region is the surface of the paper, while dark region is empty space. Each pixel represents an area  $3\mu\text{m} \times 3\mu\text{m}$

a  $3\mu\text{m} \times 3\mu\text{m}$  area on the sample and the height of the corresponding pixel on the image. As can be seen in Figure 5 the image produced by the SFG microscope clearly indicates the difference between materials (paper versus empty space). Likewise, the border of the paper is clearly seen without any blurriness or ambiguity. Thus, it is not unreasonable to assume that the SFG microscope has a resolution of at least  $3\mu\text{m}$ .

A second imaging test was performed using a human hair as a target sample. Just with the previous image, only the 532 nm laser was used. An area  $1980\mu\text{m} \times 300\mu\text{m}$  was scanned with a resolution of  $3\mu\text{m}$  between each point. The elastically scattered light was captured and a spectrum at each point was recorded. The height of the 532 nm peak was again used to determine the darkness of the image pixel corresponding to each spectrum. The resulting image, shown in Figure 6, shows the hair strand, but with less clarity than the paper edge in Figure 5. One possible cause is that the hair strand was attached to a white card, whereas for the previous image, the paper edge stood in contrast to empty space. As a background, the white card provided less contrast than empty space and thus the image of the hair strand was not as sharp as the one of the paper edge. Regardless, Figure 6 indicates that the microscope is capable of resolving objects as thin as a human hair.

## IV Conclusion

In summary, the SFG microscope has been assembled and programmed. Test acquisitions have been performed with 532 nm laser light. These tests indicate the ability of the microscope to image objects in the  $\mu\text{m}$ -range.

Future work consists of integrating the SFG microscope fully into the beamline so that SFG spectra may be taken. Then a solution of polystyrene microbeads may be used to assess the image and spectral resolution of the device. Currently, potential topics for investigation, once the microscope is complete, include the chemical degradation of explosives and the formation of soot. Since these processes deal heavily with surface chemical species, SFG microscopy is very well suited for these challenges.

Furthermore, this result indicated that the components of the SFG microscope setup—control software, xy-stage, spectrometer—are capable of operating smoothly together.

To test the imaging abilities of the microscope, the cut edge of a plain white paper card was chosen as a sample target and an acquisition was performed with just a single 532 nm laser beam. An area  $990\mu\text{m} \times 300\mu\text{m}$  was scanned with a resolution of  $3\mu\text{m}$  between each point. No SFG signal was obtained, but rather the elastically scattered 532 nm light was collected and the intensity analyzed using the spectrometer. Each spectrum represented



Figure 6: Image of a human hair taken under 532 nm laser light. Area shown is  $1980\mu\text{m} \times 300\mu\text{m}$ . The thick, dark, vertical line is the hair strand. Each pixel represents an area  $3\mu\text{m} \times 3\mu\text{m}$

## V Acknowledgments

The author would like to thank Dr. Christopher Kliewer and Brian Patterson for all their time and expertise. The author would also like to acknowledge that this work was supported in part by the U.S. Department of Energy, Office of Science, Office of Workforce Development for Teachers and Scientists (WDTS) under the Science Undergraduate Laboratory Internship (SULI) program. Likewise, this work was also supported in part by Sandia National Laboratories, a multi-program laboratory managed and operated by Sandia Corporation, a wholly owned subsidiary of Lockheed Martin Corporation, for the U.S. Department of Energy's National Nuclear Security Administration under contract DE-AC04-94AL85000.

## References

- [1] Lambert, A.G., Davies, P.B., Neivandt, D.J. Implementing the Theory of Sum Frequency Generation Vibrational Spectroscopy: A Tutorial Review. *Appl. Spectrosc. Rev.* **2005**, 40, 103-145